PVT Measurements on 4-*n*-Pentyl-4′-Cyano-Biphenyl (5CB) and trans-4-(4′-Octyl-Cyclohexyl)-Benzonitrile (8PCH) up to 300 MPa

M. Sandmann, F. Hamann, and A. Würflinger

Physical Chemistry II, Ruhr-University, D-44780 Bochum, Germany

Z. Naturforsch. **52a**, 739–747 (1997); received August 13, 1997

Specific volumes are presented for 4-*n*-pentyl-4′-cyanobiphenyl (5CB) and trans-4-(4′-octyl-cyclohexyl)-benzonitrile (8PCH) for temperatures between 300 and 370 K up to 300 MPa. The p, V_m, T data were determined for the liquid crystalline and isotropic phases, and partly also for the solid phase adjacent to the melting curve. Stable and metastable crystal phases can be distinguished. The density and melting temperature of the metastable form are lower than for the stable one. Volume and enthalpy changes accompanying the phase transitions are reported as well. The p, V_m, T data allow to calculate the entropy change for a hypothetical transition at constant volume. The molar volumes along the nematic-isotropic phase transition $T_{NI}(p)$ allow to determine the molecular field parameter $\gamma = \partial \ln T_{NI} / \partial \ln V_{NI}$.

Key words: 5CB, 8PCH, High pressure, pVT, Phase transitions, Thermodynamics, DTA.

1. Introduction

P, V_m, T measurements provide the equation of state, which is indispensable to test molecular statistical theories. Density measurements at atmospheric pressure have been performed in order to investigate pretransition effects at the NI transition and the influence of the alkyl chain length in homologous series [1–7]. Studies at atmospheric pressure have the drawback that changes of temperature and density are linked. Several authors have highlighted the advantage of constant-volume measurements which provide a better analysis of the roles of attractive and repulsive molecular interactions [8–18]. Alkylcyanobiphenyls (*n*CB) are of particular interest. They have been dielectrically investigated under pressure in [19]. Comparison of the isochoric and isobaric activation energies showed that about 50% of the molecular rotation is affected by volume effects. In the case of 5CB, p, V_m, T data were derived from refractive index measurements [18]. It seems to us that accurate volume data are better established in direct p, V_m, T measurements.

2. Experimental

The high-pressure dilatometric cell was previously developed for volume measurements on liquids and plastic crystals [20, 21]. The set-up has recently been improved by Jenau [22] and Sandmann [23]. The sample is filled in a cylindrical steel cell closed by a moving piston, whose displacement is recorded inductively, see Figure 1. In general the data are recorded along an isotherm after equilibration, starting with the highest pressure. Then the pressure is released step by step. The recorded volume changes along an isotherm are connected with the specific volumes at atmospheric pressure. Thus p, V_m, T data are established in the whole p, T range. The densities at normal pressure were determined with a commercial vibrating-tube densimeter Anton Paar DMA58.

The 5CB ($M = 249.4$ g mol^{-1}) sample was obtained from Merck and used without further purification. The 8PCH ($M = 297.5$ g mol^{-1}) sample was synthesized and purified by R. Dąbrowski in the Institute of Chemistry, Military Academy of Technology (Warsaw, Poland) and kindly provided by Professor Urban. The nematic phases were not oriented in the dilatometer.

3. Results

3.1 4-n-Pentyl-4′-Cyanobiphenyl (4′-n-pentyl-biphenyl-4-carbonitrile, 5CB)

Figure 2a shows the specific volume of 5CB as a function of pressure and temperature. The steps in the isotherms represent the volume changes at the melting (large step) and the nematic–isotropic transition (small step). Some runs at higher pressure yielded a

Reprint requests to Prof. A. Würflinger;
Fax: +49 234 70 94 183.

0932-0784 / 97 / 1000-0739 $ 06.00 © – Verlag der Zeitschrift für Naturforschung, D-72027 Tübingen

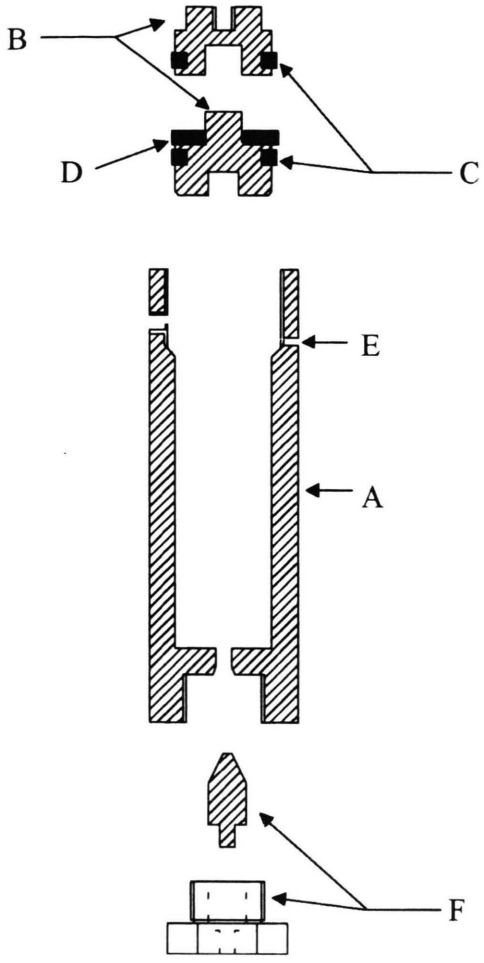

Fig. 1. Dilatometric cell for pVT measurements, A: cylindrical cell made of stainless steel, B: pistons, C: O-rings, D: indium sealing, E: gas inlet, F: cone sealing.

significantly smaller step that is attributed to the formation of a metastable crystal phase (cr′), see Figure 2 b. Metastable phases have been previously described in high-pressure DTA [24] and spectroscopic studies [25]. Literature densities at ambient pressure are available for comparison, see Figure 3. Data from Orwoll et al. [6], Sen et al. [2], Belyaev et al. [3], Dunmur and Miller [4], and Łabno et al. [26] agree well with our results, but disagree with p, V_m, T data reported by Shirakawa et al. [11]. The specific volume data are collected in detail in Table 1.

P, V_m, T data have been derived by Horn et al. from high-pressure refractive measurements with the aid of the Lorentz-Lorentz equation and special scaling factors [18]. Their data deviate by more than 1% from our results. It has been shown recently that this discrepancy causes significant errors in the evaluation of the isochoric activation energy derived from dielectic relaxation measurements [27].

The phase diagram is presented in Fig. 4, where also previous data derived from DTA measurements have been included [24, 28]. The metastable form cr′ melts at somewhat lower temperatures than the stable solid phase. The pressure dependences of the phase transition temperatures have been fitted to polynomials and are collected in Table 2.

With the use of the Clausius-Clapeyron equation we have evaluated the enthalpy and entropy changes accompanying the phase transitions. The thermodynamic results are presented in Table 3. Figure 3 shows that a pretransition effect is observed at the nematic–isotropic (NI) transition. Therefore it is difficult to determine accurate values for the NI-volume change that was also noted by Orwoll et al. [6], who report 0.0021 $cm^3\ g^{-1}$. Excluding the pretransition region, we assign a volume change of 0.45 $cm^3\ mol^{-1}$ (= 0.0018 $cm^3\ g^{-1}$ or 0.18%) to the NI transition. Dunmur et al. [4] report 0.2% for the NI transition. Clearly, the NI transition is discernible at any pressure in Fig. 2 and does not die away with increasing pressure. At higher pressures the pretransition effect is less pronounced and correspondingly we find larger values for or ΔV_{NI}. The volume and enthalpy changes, ΔV_{NI}, ΔH_{NI}, increase with rising pressure. However, the large scatter of the tabulated data shows that the accuracy is limited at higher pressures. Therefore the pressure dependence of ΔV_{NI} and ΔH_{NI} should be noted with reservation.

For the solid–nematic transition the thermodynamic changes are considerably larger. The volume change decreases significantly with increasing pressure, a normal feature of the melting process. The enthalpy change remains constant, whereas the entropy change decreases with increasing pressure. The data for the metastable form cr′ are significantly smaller. At atmospheric pressure we find $\Delta H_{cr'\text{-}N}$ = 13.82 kJ/mol, which is comparable to ΔH = 13.39 kJ/mol reported by Coles and Strazielle [29]. Porter and Schell [30] measured enthalpy changes by DSC and found 16.38 kJ/mol for the melting and 0.42 kJ/mol for the nematic–isotropic transition.

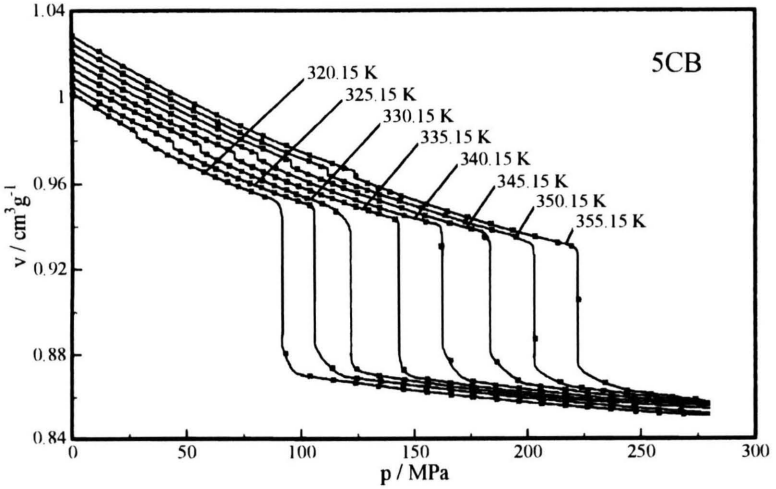

Fig. 2. a) Specific volume of 5CB as a function of pressure; the steps in the isotherms refer to the transitions: cr (stable) → nematic, nematic → isotropic.

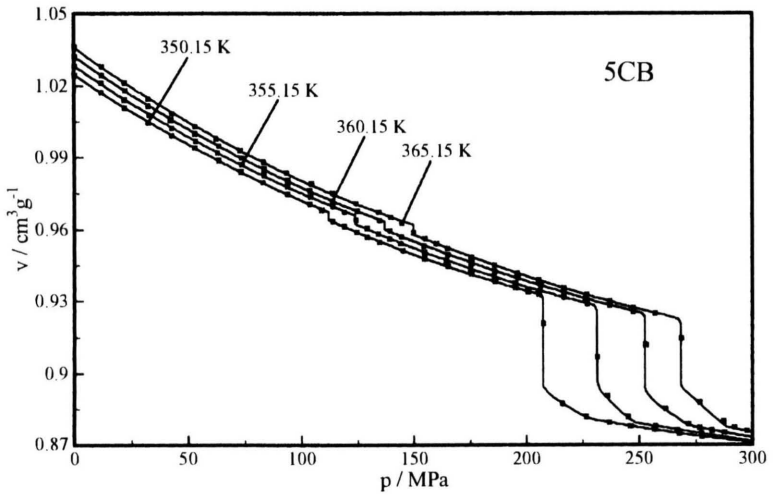

Fig. 2. b) Specific volume of 5CB as a function of pressure; the steps in the isotherms refer to the transitions: cr′ (metastable) → nematic, nematic → isotropic.

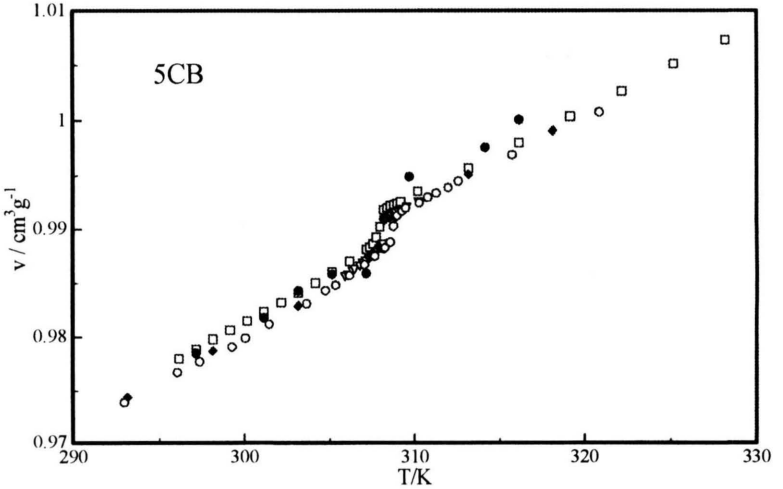

Fig. 3. Specific volume of 5CB at atmospheric pressure, (□ this work, ● Sen et al. [2], ◆ Orwoll et al. [6], ▽ Dunmur et al. [4], ○ Łabno et al. [26]).

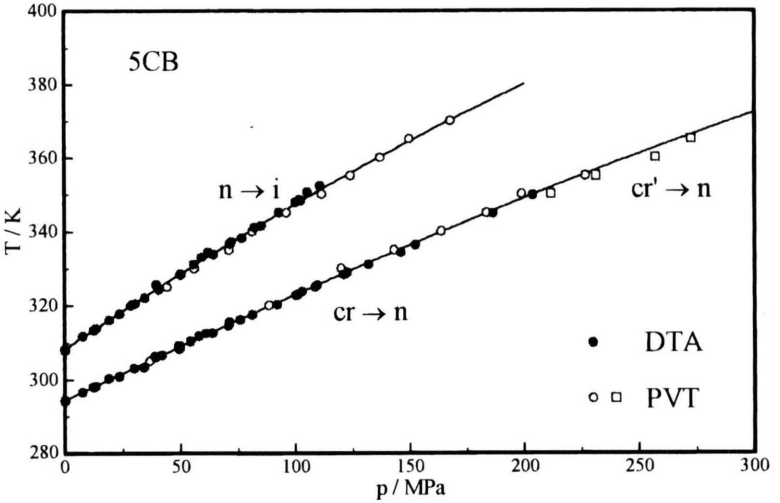

Fig. 4. Phase diagram for 5CB, (○, □ pVT, ● DTA). Melting points of the metastable form cr′ are denoted as □.

Table 1 a, b) Specific volumes ($g^{-1} \cdot cm^3$) of 5CB for the phases cr, N, and I.

p/MPa	T/K				
a)	305.15	320.15	325.15	330.15	335.15
0.1	0.986	1.001	1.005	1.009	1.013
10	0.979	0.995	0.999	1.003	1.007
20	0.973	0.989	0.993	0.997	1.001
30	0.968	0.981	0.987	0.992	0.995
40	0.874	0.975	0.982	0.986	0.990
50	0.872	0.969	0.974	0.981	0.985
60	0.870	0.965	0.968	0.073	0.980
70	0.869	0.960	0.964	0.968	0.975
80	0.867	0.956	0.959	0.963	0.967
90	0.865	0.872	0.955	0.959	0.963
100	0.864	0.871	0.952	0.955	0.959
110	0.863	0.869	0.871	0.951	0.955
120	0.861	0.868	0.870	0.873	0.951
130	0.860	0.866	0.968	0.871	0.947
140	0.859	0.865	0.867	0.869	0.944
150	0.858	0.863	0.866	0.868	0.869
160	0.856	0.862	0.864	0.866	0.868
170	0.855	0.861	0.863	0.865	0.866
180	0.854	0.860	0.862	0.863	0.865
190	0.853	0.859	0.861	0.862	0.863
200	0.852	0.858	0.860	0.861	0.862
210	0.851	0.856	0.858	0.860	0.861
220	0.850	0.856	0.857	0.859	0.860
230	0.849	0.855	0.856	0.858	0.859
240	0.849	0.845	0.856	0.857	0.858
250	0.848	0.853	0.855		0.857
260	0.847	0.852	0.854		0.856
270	0.847	0.852	0.853		0.855
280	0.846	0.851	0.852		0.854
b)	340.15	345.15	350.15	355.15	370.15
0.1	1.017	1.021	1.025	1.028	1.040
10	1.011	1.015	1.018	1.022	1.033
20	1.005	1.009	1.012	1.016	1.026
30	0.999	1.003	1.006	1.010	1.020
40	0.994	0.998	1.001	1.004	1.014
50	0.989	0.992	0.996	0.999	1.009
60	0.984	0.987	0.990	0.994	1.003
70	0.979	0.982	0.985	0.989	0.998
80	0.975	0.978	0.981	0.984	0.993
90	0.967	0.974	0.876	0.979	0.988
100	0.963	0.966	0.972	0.975	0.984
110	0.958	0.962	0.968	0.971	0.979
120	0.954	0.958	0.961	0.968	0.975
130	0.950	0.954	0.957	0.960	0.971
140	0.947	0.950	0.953	0.956	0.967
150	0.944	0.947	0.950	0.952	0.964
160	0.941	0.943	0.946	0.949	0.960
170	0.869	0.940	0.943	0.945	0.954
180	0.867	0.937	0.940	0.942	0.950
190	0.865	0.868	0.937	0.939	0.946
200	0.864	0.866	0.868	0.936	0.943
210	0.862	0.865	0.867	0.933	0.940
220	0.861	0.863	0.865	0.931	0.937
230	0.860	0.862	0.863	0.865	0.934
240	0.859	0.860	0.862	0.864	0.931
250	0.858	0.859	0.861	0.862	0.929
260	0.857	0.858	0.860	0.861	0.927
270	0.856	0.857	0.858	0.860	0.924
280	0.856	0.856	0.857	0.858	0.922

Table 1. c) Specific volumes ($g^{-1} \cdot cm^3$) of 5CB for the phases cr', N, and I.

p/MPa	T/K			
c)	350.15	355.15	360.15	365.15
0.1	1.025	1.028	1.032	1.036
10	1.018	1.022	1.026	1.029
20	1.012	1.016	1.019	1.023
30	1.006	1.010	1.013	1.016
40	1.001	1.004	1.008	1.011
50	0.996	0.999	1.002	1.005
60	0.990	0.994	0.997	1.000
70	0.985	0.989	0.992	0.994
80	0.981	0.984	0.987	0.990
90	0.976	0.979	0.982	0.985
100	0.972	0.975	0.978	0.980
110	0.968	0.971	0.974	0.976
120	0.961	0.968	0.970	0.972
130	0.957	0.960	0.966	0.969
140	0.953	0.956	0.959	0.965
150	0.950	0.952	0.955	0.958
160	0.946	0.949	0.952	0.954
170	0.943	0.945	0.948	0.951
180	0.940	0.942	0.945	0.947
190	0.937	0.939	0.941	0.944
200	0.934	0.936	0.939	0.941
210	0.935	0.933	0.936	0.937
220	0.882	0.931	0.933	0.935
230	0.881	0.928	0.930	0.932
240	0.879	0.881	0.928	0.929
250	0.877	0.879	0.925	0.927
260	0.876	0.878	0.889	0.924
270	0.875	0.876	0.878	0.881
280	0.873	0.874	0.876	0.879
290	0.872	0.873	0.875	0.877
300	0.871	0.871	0.873	0.875

Table 2. Transition temperatures as a function of pressure for 5CB and 8PCH. $T/K = a + b \cdot p/MPa + c \cdot (p/MPa)^2$.

Transition	a	b	$10^4\ c$
5CB			
cr → n	294.40	0.300	−1.33
cr' → n	280.80	0.355	−1.615
n → i	308.28	0.424	−3.20
8PCH			
cr → n	309.12	0.298	−1.874
cr' → n	305.68	0.287	−2.061
n → i	328.28	0.412	−3.613

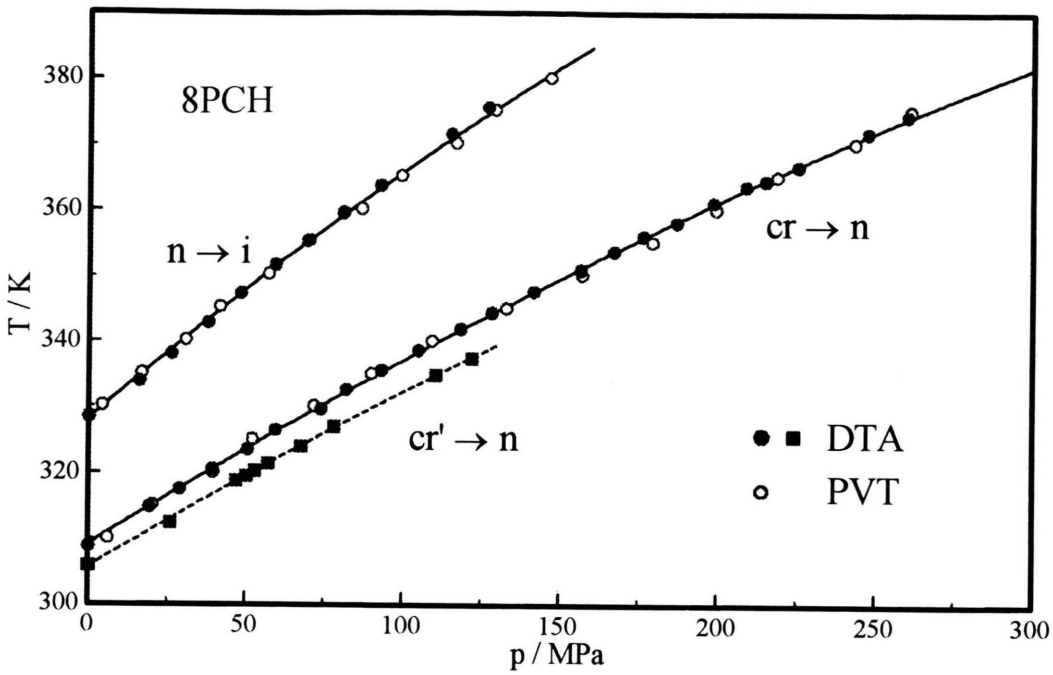

Fig. 5. Phase diagram for 8PCH, (□ pVT, ●, ■ DTA). Melting points of the metastable form cr′ are denoted as ■.

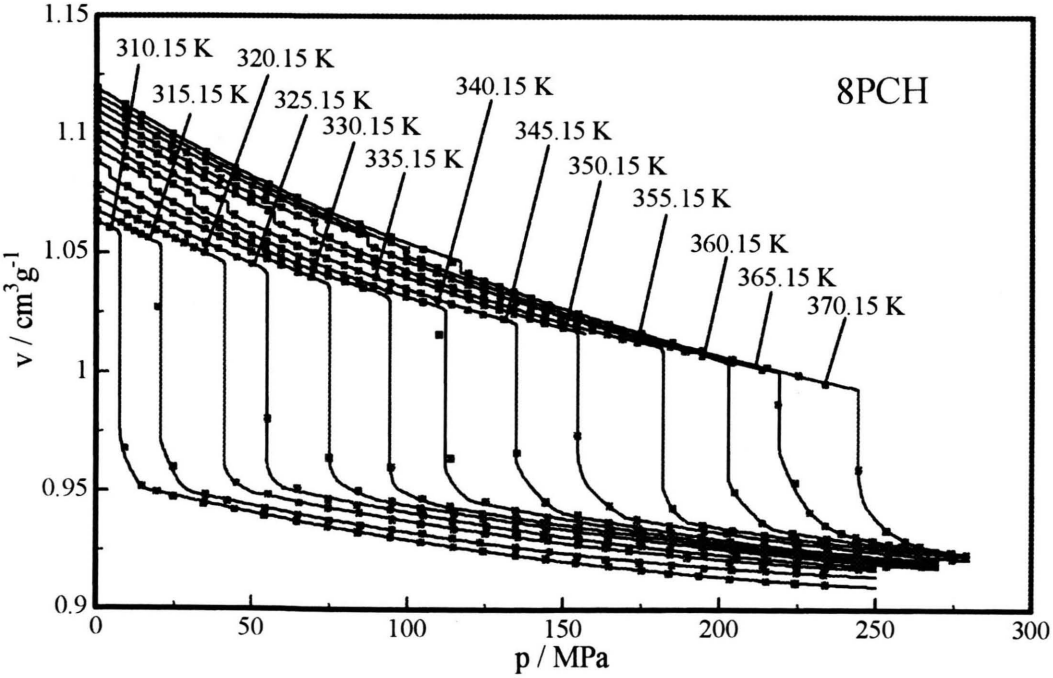

Fig. 6. Specific volume of 8PCH as a function of pressure; the steps in the isotherms refer to the transitions: cr (stable) → nematic, nematic → isotropic.

Table 3. Thermodynamic properties of 5CB.

Phase transition	T/ K	p/ MPa	ΔV_m/ ($cm^3 \cdot mol^{-1}$)	ΔH_m/ ($kJ \cdot mol^{-1}$)	ΔS_m/ ($J \cdot mol^{-1} \cdot K^{-1}$)
$n \rightarrow i$	308.05	0.1	0.45	0.33	1.1
	320.15	28.4	0.54	0.43	1.3
	325.15	44.2	0.75	0.62	1.9
	330.15	55.9	0.69	0.58	1.8
	335.15	70.9	0.79	0.70	2.1
	340.15	81.1	0.64	0.58	1.7
	345.15	96.1	0.70	0.67	1.9
	350.15	111.5	0.79	0.79	2.2
	355.15	124.1	0.89	0.93	2.6
	360.15	137.0	0.85	0.91	2.5
	365.15	149.7	1.03	1.14	3.2
	370.15	167.7	0.85	1.00	2.7
cr $\rightarrow n$	294.50	0.1	23.2	22.55	76.6
	305.15	36.7	21.9	22.90	75.1
	320.15	88.5	20.1	23.32	72.8
	235.15	108.7	19.4	23.38	71.9
	330.15	119.9	19.1	23.67	71.7
	335.15	143.1	18.3	23.66	70.6
	340.15	163.7	17.5	23.53	69.2
	345.15	183.5	16.9	23.62	68.4
	350.15	198.8	16.3	23.56	67.3
	355.15	226.8	15.4	23.40	65.9
cr′ $\rightarrow n$	281.90	0.1	17.4	13.82	49.0
	350.15	211.6	11.9	14.54	41.5
	355.15	231.4	11.5	14.57	41.0
	360.15	257.2	10.9	14.44	40.1
	365.15	272.6	10.3	14.09	38.6

3.2 Trans-4-(4′-Octyl-Cyclohexyl)-Benzonitrile (or trans-4-n-octyl-(4′-cyanophenyl)-cyclohexane, 8PCH)

The phase diagram of 8PCH presented in Fig. 5 was established both by differential thermal analysis [31] and volume measurements [23]. In the DTA study the melting was sometimes considerably shifted to lower temperatures. This lower transition disappeared after appropriate annealing. The lower melting curve is presented in the Figure as a dashed line and is apparently related to a metastable crystal phase cr′. Haase et al. [32] denote the stable form as PCH8A and the metastable form as PCH8B. The lower melting curve was not detected in the pVT measurements. The transition temperatures are included in Table 2. At atmospheric pressure there is good agreement with data from Haase et al. [32] and Kędziora et al. [33].

Figure 6 shows the specific volumes as a function of pressure for different isotherms. As for 5CB, the nematic–isotropic transition is clearly discernable. The specific volume data are collected in Table 4 and the thermodynamic quantities in Table 5. As was found for 5CB, the ΔV_{NI} and ΔH_{NI} values increase with rising pressure, whereas $\Delta V_{cr\text{-}N}$ and $\Delta H_{cr\text{-}N}$ decrease. Haase et al. [32] have calculated densities for the crystal phase from X-ray measurements, which agree well with the present work. They determined the enthalpy change on melting with DSC: $\Delta H = 37$ kJ/mol for PCH8A and 32 kJ/mol for PCH8B. With the use of our volume data we calculate $\Delta H = 33.3$ kJ/mol, which agrees better with PCH8B. However, the melting transition was observed at 308.85 K that corresponds to PCH8A.

Only high pressure data for 3PCH, 5PCH and 7PCH are available for comparison [16]. Similarly to results for 5PCH and 7PCH [16] we observe in the neighbourhood of the nematic–isotropic transition larger compressibilities for the nematic phase than for the isotropic phase.

4. Discussion

The entropy change, ΔS_{tr}, at a first-order phase transition can be split into a constant-volume (or configurational) part, and a dilational part [22]. The latter can be evaluated with the help of p, V_m, T data:

$$\Delta S_{tr} = \Delta S_{conf} + (\partial S/\partial V)_T \Delta V_{tr}$$
$$= \Delta S_{conf} + (\partial p/\partial T)_V \Delta V_{tr} .$$

We denote the constant volume entropy ($\Delta S_{tr,V}$ in [6]) as ΔS_{conf}, because this entropy part is usually related to configurational changes at constant volume. Combining this expression with the Clausius-Clapeyron equation $(\partial p/\partial T)_{tr} = \Delta S_{tr}/\Delta V_{tr}$ we obtain

$$\Delta S_{conf} = [(\partial p/\partial T)_{tr} - (\partial p/\partial T)_V] \Delta V_{tr}$$

or

$$\Delta S_{conf}/\Delta S_{tr} = [(\partial p/\partial T)_{tr} - (\partial p/\partial T)_V]/(\partial p/\partial T)_{tr} .$$

Orwoll et al. [6] and Horn et al. [18] have applied this procedure to the evaluation of the constant volume entropy for 5CB. They found approximately 50% for the ratio $\Delta S_{conf}/\Delta S_{tr}$. A similar result was found by Abe et al. [14] for α,ω-bis[(4,4′-cyanobiphenylyl)oxy]-alkanes. Using our high-pressure data we find an increasing ratio (~ 0.4 to 0.6) with rising pressure, see Figure 7. According to this finding only half of the total entropy change ΔS_{NI} can be associated to the change of the order parameter. This might be useful to elucidate phase transition theories [34].

Several authors [8–13] have investigated the pressure dependence of the nematic $\rightarrow$ isotropic phase

Table 4. a) Specific volumes ($g^{-1} \cdot cm^3$) of 8PCH for the phases cr, N, and I.

p/MPa	T/K						
	310.15	315.15	320.15	325.15	330.15	335.15	340.15
0.1	1.063	1.068	1.073	1.078	1.088	1.093	1.098
10	0.953	1.061	1.066	1.071	1.077	1.086	1.090
20	0.949	1.053	1.059	1.064	1.070	1.075	1.082
30	0.946	0.949	1.053	1.057	1.063	1.067	1.074
40	0.944	0.947	1.047	1.050	1.056	1.060	1.064
50	0.941	0.944	0.949	1.045	1.050	1.053	1.057
60	0.939	0.941	0.947	0.951	1.046	1.048	1.051
70	0.936	0.939	0.944	0.948	1.039	1.042	1.046
80	0.934	0.937	0.942	0.946	0.952	1.038	1.041
90	0.932	0.935	0.940	0.943	0.946	1.034	1.036
100	0.929	0.933	0.937	0.941	0.944	0.949	1.032
110	0.927	0.931	0.935	0.939	0.942	0.944	0.950
120	0.926	0.929	0.933	0.937	0.940	0.942	0.946
130	0.924	0.927	0.932	0.935	0.938	0.940	0.943
140	0.922	0.925	0.930	0.933	0.936	0.938	0.941
150	0.920	0.924	0.928	0.931	0.934	0.936	0.938
160	0.919	0.922	0.927	0.929	0.932	0.934	0.936
170	0.918	0.921	0.925	0.927	0.930	0.932	0.934
180	0.916	0.920	0.924	0.926	0.929	0.930	0.932
190	0.915	0.919	0.922	0.925	0.927	0.929	0.930
200	0.914	0.918	0.921	0.923	0.926	0.927	0.928
210	0.913	0.917	0.920	0.922	0.924	0.926	0.927
220	0.912	0.916	0.919	0.921	0.923	0.924	0.925
230	0.911	0.915	0.918	0.920	0.922	0.923	0.924
240	0.910	0.915	0.918	0.919	0.921	0.922	0.923
250	0.910	0.914	0.917	0.918	0.920	0.921	0.922
260					0.919	0.919	0.921
270					0.918	0.918	0.920

Table 4. b) Specific volumes ($g^{-1} \cdot cm^3$) of 8PCH for the phases cr, N, and I.

p/MPa	T/K					
	345.15	350.15	355.15	360.15	365.15	370.15
0.1	1.102	1.106	1.110	1.113	1.116	1.119
10	1.094	1.098	1.102	1.106	1.109	1.111
20	1.086	1.091	1.095	1.098	1.101	1.103
30	1.079	1.084	1.088	1.091	1.094	1.096
40	1.072	1.077	1.081	1.085	1.087	1.089
50	1.062	1.071	1.074	1.078	1.080	1.082
60	1.056	1.061	1.068	1.072	1.074	1.076
70	1.050	1.055	1.059	1.066	1.068	1.070
80	1.045	1.050	1.053	1.061	1.062	1.064
90	1.039	1.045	1.047	1.052	1.057	1.059
100	1.035	1.040	1.042	1.046	1.049	1.054
110	1.030	1.035	1.037	1.041	1.044	1.050
120	1.026	1.030	1.033	1.037	1.039	1.041
130	1.023	1.026	1.029	1.032	1.034	1.036
140	0.947	1.022	1.025	1.028	1.029	1.031
150	0.941	1.019	1.021	1.024	1.025	1.027
160	0.938	0.945	1.017	1.020	1.021	1.023
170	0.936	0.939	1.014	1.016	1.017	1.018
180	0.934	0.937	0.942	1.013	1.013	1.014
190	0.932	0.935	0.937	1.009	1.010	1.011
200	0.930	0.933	0.935	0.945	1.006	1.007
210	0.928	0.931	0.933	0.938	1.003	1.004
220	0.926	0.929	0.931	0.933	0.941	1.000
230	0.925	0.927	0.929	0.931	0.936	0.997
240	0.924	0.926	0.928	0.929	0.932	0.994
250	0.923	0.925	0.926	0.928	0.929	0.934
260	0.922	0.923	0.925	0.926	0.927	0.928
270	0.921	0.922	0.924	0.924	0.925	0.925
280		0.921	0.923	0.923	0.924	0.924

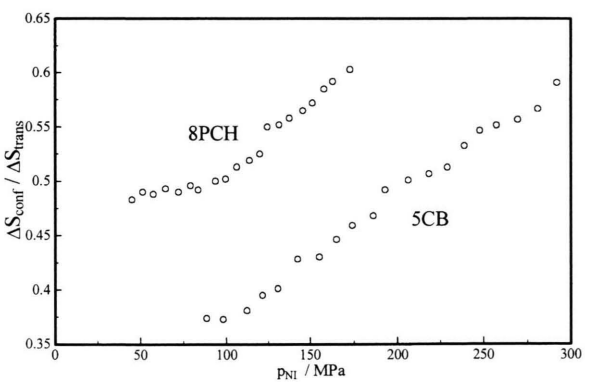

Fig. 7. Entropy separation for the nematic → isotropic transition for 5CB, and 8PCH.

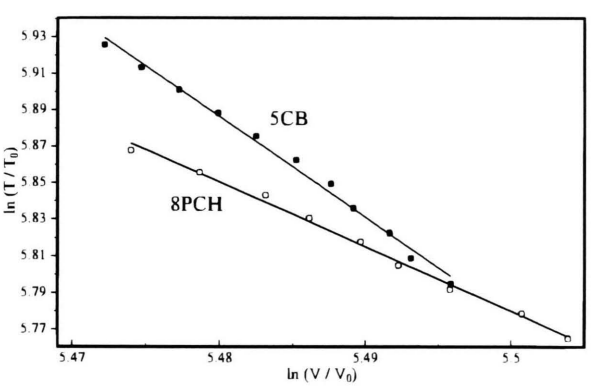

Fig. 8. Logarithm of the clearing temperature against the logarithm of the molar volume as a function of pressure for 5CB and 8PCH, T_0 and V_0 refer to atmospheric pressure.

Table 5. Thermodynamic properties of 8PCH.

Phase transition	T/ K	p/ MPa	ΔV_m/ ($cm^3 \cdot mol^{-1}$)	ΔH_m/ ($kJ \cdot mol^{-1}$)	ΔS_m/ ($J \cdot mol^{-1} \cdot K^{-1}$)
$n \rightarrow i$	328.45	0.1	0.82	0.65	2.0
	330.15	4.3	1.08	0.87	2.6
	335.15	16.7	1.07	0.89	2.7
	340.15	30.7	1.15	1.00	2.9
	345.15	41.5	1.18	1.06	3.1
	350.15	57.1	1.26	1.19	3.4
	355.15	69.6	1.23	1.21	3.4
	360.15	86.6	1.05	1.06	3.0
	365.15	99.2	0.88	0.94	2.6
	370.15	116.6	1.37	1.55	4.2
	375.15	129.0	1.31	1.54	4.1
	380.15	146.5	1.14	1.41	3.7
cr $\rightarrow$ n	308.85	0.1	32.3	33.3	107.7
	310.15	6.2	31.2	32.8	105.6
	315.15	20.3	30.2	32.7	103.1
	320.15	39.6	28.3	32.0	99.8
	325.15	52.3	27.0	31.6	97.1
	330.15	71.8	24.6	29.9	90.7
	335.15	90.0	23.7	30.1	89.8
	340.15	109.2	23.0	30.4	89.4
	345.15	132.8	21.0	29.3	84.8
	350.15	156.9	20.8	30.4	86.9
	355.15	179.2	19.8	30.4	85.7
	360.15	199.4	17.9	28.9	80.3
	365.15	218.7	17.0	29.8	81.6
	370.15	243.4	15.7	28.1	76.0
	375.15	261.2	15.4	29.2	77.8

transition in order to determine the slope $\gamma = \partial \ln T_{NI} / \partial \ln V_{NI}$, which is related to the molecular field potential. From a corresponding plot (Fig. 8) we derive $\gamma = 5.3$ for 5CB and $\gamma = 3.4$ for 8PCH. In agreement with previous findings, the *n*PCH series yields smaller values for γ than the *n*CBs [19]. The large value of γ indicates that both the attractive and repulsive must be taken into account. In the Maier-Saupe theory only the attractive part was considered, corresponding to $\gamma = 2$.

High-pressure studies are useful to investigate the phase situation. With the knowledge of the equation of state one can distinguish between isochoric temperature changes and isothermal density change. This gives more insight in the role of molecular interactions.

Acknowledgements

Grants from the Deutsche Forschungsgemeinschaft (Wu 97/10-1) and Fonds der Chemischen Industrie are gratefully acknowledged. We appreciate also financial support in the frame of an exchange program between the Ruhr-Universität Bochum and the Uniwersytet Jagielloński Kraków and discussions with Professor Urban.

[1] D. Demus, A. Hauser, A. Isenberg, M. Pohl, C. Selbmann, W. Weissflog, and S. Wieczorek, Cryst. Res. Technol. **20,** 1413 (1985).
[2] S. Sen, P. Brahma, S. K. Roy, D. K. Mukherjee, and S. B. Roy, Mol. Cryst. Liq. Cryst. **100,** 327 (1983).
[3] V. V. Belyaev, M. F. Grebenkin, and V. F. Petrov, Russ. J. Phys. Chem. **64,** 509 (1990).
[4] D. A. Dunmur and W. H. Miller, J. Physique Coll. C3, **40,** 141 (1979). W. H. Miller, thesis.
[5] S. Lakshminarayana, C. R. Prabhu, D. M. Potukuchi, N. V. S. Rao, V. G. K. M. Pisipati, and D. Saran, Liq. Cryst. **15,** 909 (1993).
[6] R. A. Orwoll, V. J. Sullivan, and G. C. Campbell, Mol. Cryst. Liq. Cryst. **149,** 121 (1987).
[7] A. J. Leadbetter, J. L. A. Durrant, and M. Rugman, Mol. Cryst. Liq. Cryst. Lett. **34,** 231 (1977).
[8] J. R. McColl and C. S. Shih, Phys. Rev. Lett. **29,** 85 (1972).
[9] R. V. Tranfield and P. J. Collings, Phys. Rev. A **25,** 2744 (1982); C. S. Johnson and P. J. Collings, J. Chem. Phys. **79,** 4056 (1983).
[10] H. Ichimura, T. Shirakawa, T. Tokuda, and T. Seimiya, Bull. Chem. Soc. Japan **56,** 2238 (1983).
[11] T. Shirakawa, T. Hayakawa, and T. Tokuda, J. Phys. Chem. **87,** 1406 (1983); T. Shirakawa, T. Inoue, and T. Tokuda, J. Phys. Chem. **86,** 1700 (1982).
[12] T. Shirakawa, M. Arai, and T. Tokuda, Mol. Cryst. Liq. Cryst. **104,** 131 (1984).
[13] W. M. Lampe and P. J. Collings, Phys. Rev. A **34,** 524 (1986).
[14] A. Abe and S. Y. Nam, Macromolecules **28,** 90 (1995).
[15] R. Shashidhar, P. H. Keyes, and W. B. Daniels, Mol. Cryst. Liq. Cryst. Lett. **3,** 169 (1986); P. H. Keyes and W. B. Daniels, J. Physique Coll. **C3,** 380 (1979).
[16] E. Kuss, Mol. Cryst. Liq. Cryst. **76,** 199 (1981).
[17] H. Allouchi, P. Kromm, J. P. Bideau, M. Cotrait, C. Destrade, H. T. Nguyen, and D. Guillon, JEEP, France (1994).
[18] R. G. Horn and T. E. Faber, Proc. Roy. Soc. A **368,** 199 (1979); R. G. Horn, J. Phys. Paris **39,** 167 (1978).
[19] S. Urban and A. Würflinger, Adv. Chem. Phys. **98,** 143 (1997).
[20] R. Landau and A. Würflinger, Rev. Sci. Instrum. **51,** 533 (1980).
[21] M. Riembauer, L. Schulte, and A. Würflinger, Z. Phys. Chem. Frankfurt, N.F. **166,** 53 (1990).
[22] M. Jenau, Doctoral Thesis, Ruhr-University of Bochum 1996; M. Jenau and A. Würflinger, Z. Physik. Chem. Frankfurt **199,** 255 (1997).
[23] M. Sandmann, Doctoral Thesis, Ruhr-University of Bochum, in preparation.
[24] M. Hartmann, M. Jenau, A. Würflinger, M. Godlewska, and S. Urban, Z. Phys. Chem. Frankfurt **177,** 195 (1992).
[25] H. C. Hsueh, H. Vass, F. N. Pu, S. J. Clark, W. C. K. Poon, and J. Crain, Europhysics Letters **38,** 107 (1997).

[26] W. Łabno and J. Jadżyn, Pr. Kom. Mat.-Przyr., Poznan, Tow. Przyj. Nauk, Fiz. Dielektr. Radiospektrosk. **12,** 75 (1981).
[27] M. Sandmann, D. Büsing, T. Brückert, A. Würflinger, S. Urban, and B. Gestblom, SPIE 97 (Zakopane).
[28] M. Hugo, Diplom Thesis, Bochum 1991.
[29] H. J. Coles and C. Strazielle, Mol. Cryst. Liq. Cryst. **55,** 237 (1979).
[30] R. S. Porter and K. T. Schell, Mol. Cryst. Liq. Cryst. **182 B,** 185 (1990).
[31] F. Hamann, Doctoral Thesis, Ruhr-University of Bochum, in preparation.
[32] W. Haase, J. Loub, H. Paulus, M. A. Mokhles, and I. H. Ibrahim, Mol. Cryst. Liq. Cryst. **197,** 47 (1991); H. Paulus and W. Haase, Mol. Cryst. Liq. Cryst. Lett. **92,** 237 (1983).
[33] P. Kędziora and J. Jadżyn, Mol. Cryst. Liq. Cryst. **249,** 105 (1994).
[34] J. Thoen, Int. J. Mod. Phys. B **9,** 2157 (1995).